Counterion and Solvation Effects on the Conformations of the Radical Anions of 2,5-Dicyanovinyl Substituted Furan and Thiophene. An EPR and ENDOR Study

Markus Scholz,[a] Georg Gescheidt,*[,a] Ulrich Schöberl[b] and Jörg Daub[b]
[a] *Institut für Physikalische Chemie, Universität Basel, Klingelbergstrasse 80, CH 4056 Basel, Switzerland*
[b] *Institut für Organische Chemie, Universität Regensburg, Universitätsstrasse 31, D 8400 Regensburg, Germany*

The radical anions of two tetranitrile compounds, *i.e.*, 2,2'-(furan-2,5-diyldimethylidene)-bispropanedinitrile (**1**) and 2,2'-(thiophene-2,5-diyldimethylidene)bispropanedinitrile (**2**), have been investigated in a 1,2-dimethoxyethane/*N,N,N',N',N'',N''*-hexamethylphosphoric triamide mixture, 1,2-dimethoxyethane, tetrahydrofuran, and 2-methyltetrahydrofuran as the solvents and with Li^+, Na^+, K^+, Cs^+ as the counterions and in *N,N*-dimethylformamide with Zn^{2+} as counterion. A remarkable dependence of the molecular symmetry upon ion-pair formation is found for both molecules. The symmetry of both radical anions increases to C_{2v} under conditions favouring contact ion-pair formation.

Low-molecular-weight carbohydrates were used as source compounds for the synthesis of 2,2'-(furan-2,5-diyldimethylidene)bispropanedinitrile (**1**) and 2,2'-(thiophene-2,5-diyldimethylidene)bispropanedinitrile (**2**).[1] Recently, the redox properties of **1** were reported and compared to those of the thiophene derivative **2**.[2] It was shown that **1** and **2** can be reduced to their radical anions and dianions in two distinct reversible steps at −890 and −1240 mV (**1**; *vs.* ferrocene) and −808 and −1174 mV (**2**), respectively. This 'easy' uptake of electrons is in line with an electronic structure of **1** and **2** where both dicyanomethylidene groups are part of a planar conjugated π-system. However, these two molecules may possess more than just one planar structure. Whereas a nearly planar solid-state structure of C_{2v} symmetry of **1** was established by X-ray crystal structure analysis,[1] three planar conformations of **1** and **2** or their radical anions which favour delocalization are to be taken into account in solution (Fig. 1): two of them have C_{2v} (*syn/syn* and *anti/anti*) and one C_s symmetry (*syn/anti*). The notations *syn* and *anti* refer to the dicyanomethylidene moieties being oriented towards the furan O-atoms or the thiophene S-atoms (*syn*) or in the opposite direction (*anti*).

The effects of electron transfer on the geometry of molecules have already been subject to investigations.[3] The model of ion pairing in radical anions was mainly elaborated by Hirota[4] and the knowledge of radical-ion pairs up to 1971 was reported in two books edited by Szwarc.[5] The influence of alkali-metal association on twisting around single bonds in radical anions[6] and on the spin distribution in radical anions[7,8] was reported. A contribution dealing with conformations of furan and thiophene-2- and -3-carbaldehydes[9a] gave no evidence of counterion effects whereas for thiophene-2,5-dicarbaldehyde an ion pair leading to a decrease of the C_{2v} molecular symmetry to C_s was established.[9b]

In this study we want to focus on the conformational changes of the radical anions $\mathbf{1}^{\bullet-}$ and $\mathbf{2}^{\bullet-}$ depending on solvation and the nature of the alkali-metal counterion as indicated by EPR, ENDOR[10] (Electron Nuclear DOuble Resonance) and TRIPLE-resonance[11] spectroscopy.

Experimental

The radical anions $\mathbf{1}^{\bullet-}$ and $\mathbf{2}^{\bullet-}$ were generated by chemical reduction of the neutral compounds at 203 K. Na, K, Cs and Zn were used as reducing agents; LiCl was added, when Li^+ was the desired counterion. A mixture of *N,N,N',N', N'', N''*-hexamethylphosphoric triamide (HMPA)/1,2-dimethoxyethane (DME) 1:5, *N,N*-dimethylformamide (DMF), DME, tetrahydrofuran (THF), and 2-methyltetrahydrofuran (MTHF) served as solvents. The radical anions $\mathbf{1}^{\bullet-}$ and $\mathbf{2}^{\bullet-}$ were investigated in the temperature range between the freezing points of the solvents and the decay of the EPR spectra at higher temperatures (*ca.* 270 K).

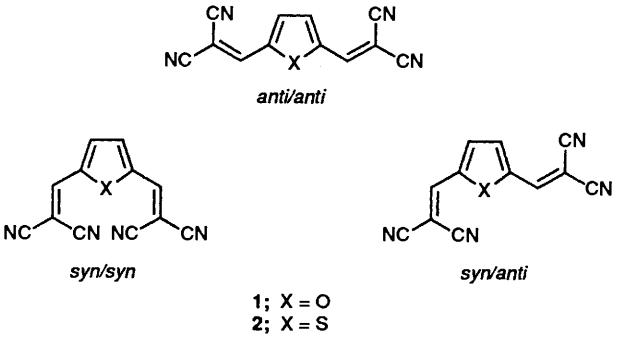

Fig. 1 Three possible planar conformations of **1** and **2**

For EPR measurements, a Varian E-9 spectrometer was used. ENDOR and TRIPLE-resonance spectra were taken on a Bruker ESP 300 spectrometer system.

Results

EPR and ENDOR Spectra.—Three distinct types of EPR and ENDOR spectra were detected, when counterion, solvent, and the temperature of the samples containing $\mathbf{1}^{\bullet-}$ and $\mathbf{2}^{\bullet-}$ were varied. As demonstrated by the following examples, the types of spectra are denoted as *A*, *S* and *M*.

(i) Fig. 2 (top) shows the EPR spectrum (type *A*) of $\mathbf{1}^{\bullet-}/Cs^+$ in DME at 203 K. In this spectrum type, no central line exists and the low- and the high-field halves show identical patterns. The corresponding ENDOR spectrum consists of eight signals belonging to four ^1H coupling constants [Fig. 2, (bottom)].

(ii) A second kind of EPR spectrum (Fig. 3, type *S*), *e.g.* that of $\mathbf{2}^{\bullet-}/Na^+$ (MTHF, 243 K), consists of a pattern with a central line and matching low- and high-field halves. The ENDOR spectrum indicates four signals belonging to two ^1H coupling constants.

(iii) In Fig. 4, EPR and ENDOR spectra of $\mathbf{1}^{\bullet-}/K^+$ (DME,

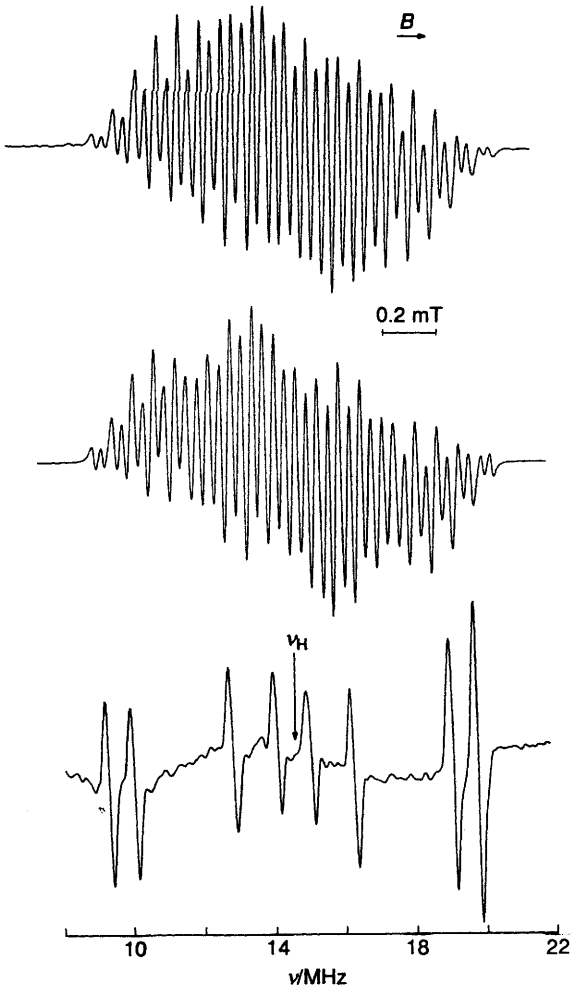

Fig. 2 Top: EPR-spectrum of the radical anion $\mathbf{1}^{\bullet -}$; solvent, DME; temperature, 203 K; counterion; Cs^+, middle: computer simulation, bottom: corresponding proton ENDOR spectrum (type *A*)

223 K, type *M*) are displayed. As in the EPR spectrum of type *A*, there is no central line, but the low- and the high-field halves do not correspond. The ENDOR spectrum shows 12 signals belonging to six ^1H coupling constants and represents a superposition of spectra of type *A* and *S*.

Determination of the Hyperfine Coupling Constants.—The ^1H coupling constants for the simulation of the EPR spectra were taken from ENDOR or special-TRIPLE-resonance experiments. General-TRIPLE-resonance spectra indicate the same sign for all ^1H-coupling constants. According to the HMO–McLachlan[12] calculations this sign is negative, as expected for H-atoms directly bound to the sp^2-hybridized C-atoms bearing π-spin population (α-protons). The ^{14}N coupling constants could not be detected by the ENDOR technique and were therefore deduced from the EPR spectra. The protons at the dicyanoethene moieties of the molecules are abbreviated with H_e, those at the furan or thiophene ring with H_f. In Tables 1–5, the a_{He} and a_{Hf} values of $\mathbf{1}^{\bullet -}$ are given for Li^+, Na^+, K^+ and Cs^+ as counterions and HMPA/DME, DME, THF and MTHF as solvents at four different temperatures. The values determined upon reduction with Zn in a DMF solution were identical to those recorded in HMPA/DME. The *g* factor of the EPR spectra of $\mathbf{1}^{\bullet -}$ is 2.0029 ± 0.0001 throughout. An overview of some relevant EPR data of $\mathbf{2}^{\bullet -}$ is given in Table 6 (g = 2.0038 ± 0.0001).

Assignment of Coupling Constants.—In accord with the favoured (see Introduction) planar structure of $\mathbf{1}^{\bullet -}$ and $\mathbf{2}^{\bullet -}$,

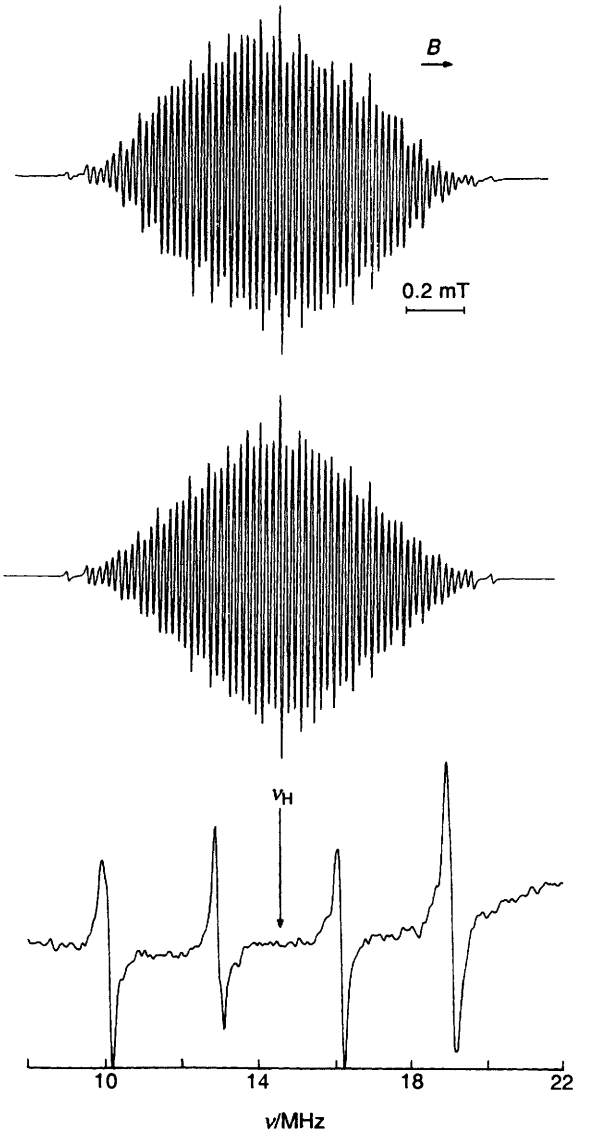

Fig. 3 Top: EPR-spectrum of the radical anion $\mathbf{2}^{\bullet -}$; solvent, MTHF; temperature, 243 K; counterion; Na^+, middle: computer simulation, bottom: corresponding proton ENDOR spectrum (type *S*)

HMO calculations were performed to evaluate the ^1H coupling constants. The following 'heteroatom parameters' for the N-atoms were used: 1.0 for h_N, and 2.0 for k_{CN} (C, N triple bond), where $\alpha' = \alpha + h\beta$ and $\beta' = k\beta$. The parameters for the O-atom[13] and the S-atom[14] were set to h_O = 2.0, k_{CO} = 1.0 and h_S = 1, k_{CS} = 0.65, both, O and S, contributing two electrons to the π-system.[15] Thus, $\mathbf{1}^{\bullet -}$ and $\mathbf{2}^{\bullet -}$ are to be regarded as 19-electron π-systems. In Fig. 5, the lowest unoccupied molecular orbital (LUMO) of **1**, representing the spin distribution in the radical anions, is shown together with the HMO–McLachlan[12] calculated ^1H hyperfine-coupling constants of $\mathbf{1}^{\bullet -}$; the corresponding values of $\mathbf{2}^{\bullet -}$ are given in parentheses. According to the calculated values, the a_H of *ca.* 0.34 mT ($\mathbf{1}^{\bullet -}$, calc. 0.35) and 0.30 mT ($\mathbf{2}^{\bullet -}$, calc. 0.29) (Tables 1–6) were assigned to the two protons at the dicyanoethene moieties (H_e) and those of *ca.* 0.1 mT ($\mathbf{1}^{\bullet -}$, calc. 0.07; $\mathbf{2}^{\bullet -}$, calc. 0.10) to the two protons at the furan/thiophene ring (H_f). The decrease of a_{He} in $\mathbf{2}^{\bullet -}$ as compared to $\mathbf{1}^{\bullet -}$ is in line with the calculations (Fig. 5). The spin populations of 0.038 ($\mathbf{1}^{\bullet -}$ and $\mathbf{2}^{\bullet -}$) at the four N-atoms are reflected by the ^{14}N coupling constants, a_N, lying between 0.06 and 0.09 mT. The differences between these a_N values are in the same order of magnitude as the EPR line-width, hence it is impracticable to discern the

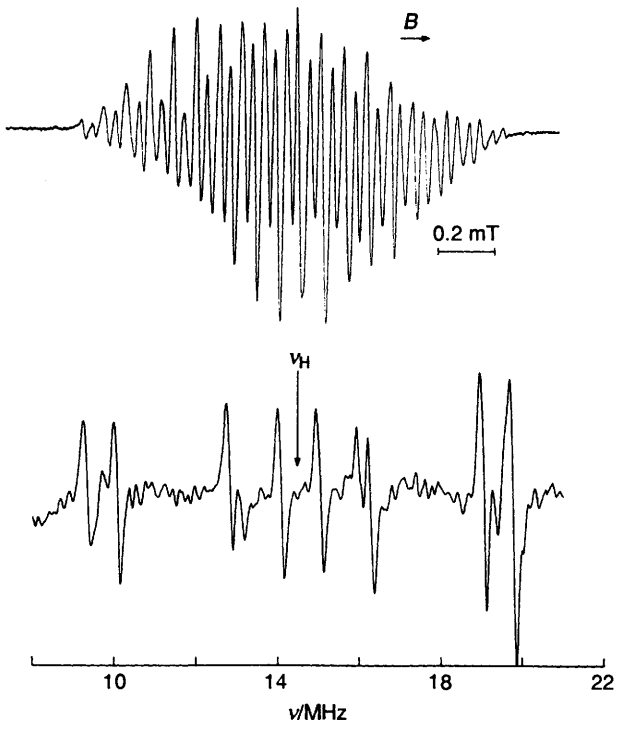

Fig. 4 Top: EPR-spectrum of the radical anion $\mathbf{1}^{\bullet -}$; solvent, DME; temperature, 223 K; counterion; K^+, bottom: corresponding proton ENDOR spectrum (type *M*)

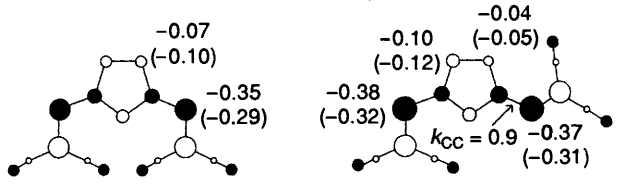

Fig. 5 Lowest unoccupied orbitals (LUMO) of **1** for C_{2v} (left) and C_s (right) symmetry; the numbers indicate the HMO–McLachlan calculated ^1H hyperfine coupling constants (in mT) for $\mathbf{1}^{\bullet -}$ and $\mathbf{2}^{\bullet -}$ (in parentheses)

Table 1 ^1H Coupling constants of $\mathbf{1}^{\bullet -}$ (mT). Solvent: DME/HMPA 5:1; counterion; K^+ or Cs^+

T/K	$a(H_e)$	$a(H_f)$	EPR-Type
203	0.382, 0.314	0.130, 0.026	*A*
223	0.378, 0.311	0.128, 0.026	*A*
243	0.371, 0.309	0.126, 0.029	*A*
263	0.365, 0.307	0.123, 0.030	*A*

coupling constants of the symmetrically non-equivalent N-atoms.

To mimic the change of the conformations from *syn/syn* or *anti/anti* (C_{2v}) to *syn/anti* (C_s) (Fig. 1), the parameter for the bond connecting the five-membered ring and one dicyanoethene moiety, k_{CC}, was changed to 0.9.* Thus, the coupling constants were split into 0.37 and 0.38 mT for H_e of $\mathbf{1}^{\bullet -}$ ($\mathbf{2}^{\bullet -}$, 0.31 and 0.32 mT) and 0.04 and 0.10 mT for H_f ($\mathbf{2}^{\bullet -}$, 0.05 and 0.12 mT) as shown in Fig. 5 (right part). This behaviour parallels the experimental results (Tables 1–6).

* The small change of the parameter k_{CC} from 1.0 for a planar π-system to 0.9 is, in this case, not due to a deviation from planarity but represents the decrease of the symmetry in **1** or **2** on going from the *syn/syn* or *anti/anti* conformations to the *syn/anti* (Fig. 1).

Table 2 ^1H Coupling constants of $\mathbf{1}^{\bullet -}$ (mT). Counterion: Li^+, solvents: DME, THF, MTHF

T/K	$a(H_e)$	$a(H_f)$	EPR-type
	DME		
203	0.370, 0.318	0.122, 0.034	*A*
223	0.368, 0.317	0.106, 0.033	*A*
243	0.364, 0.317	0.103, 0.033	*M*[a]
263	0.362	0.101	*S*
	THF		
203	0.369, 0.319	0.119, 0.035	*A*
223	0.369, 0.319	0.119, 0.035	*A*
243	0.370, 0.317	0.102, 0.039	*M*[a]
263	0.366	0.102	*S*
	MTHF		
203	0.369	0.101	*S*
223	0.369	0.101	*S*
243	0.369	0.101	*S*
263	0.369	0.101	*S*

[a] Spectrum type derived from EPR, in the ENDOR spectrum two pairs of lines were not resolved.

Table 3 ^1H Coupling constants of $\mathbf{1}^{\bullet -}$ (mT). Counterion: Na^+, solvents: DME, THF, MTHF

T/K	$a(H_e)$	$a(H_f)$	EPR-type
	DME		
203	0.367, 0.349, 0.321	0.126, 0.102, 0.035	*M*
223	0.362, 0.347, 0.320	0.124, 0.101, 0.035	*M*
243	0.356, 0.342, 0.319	0.123, 0.101, 0.035	*M*
263	0.352	0.100	*S*
	THF		
203	0.351	0.101	*S*
223	0.346	0.098	*S*
243	0.343	0.098	*S*
263	0.340	0.097	*S*
	MTHF		
203	0.352	0.101	*S*
223	0.350	0.099	*S*
243	0.347	0.099	*S*
263	0.343	0.099	*S*

Table 4 ^1H Coupling constants of $\mathbf{1}^{\bullet -}$ (mT). Counterion: K^+, solvents: DME, THF, MTHF.

T/K	$a(H_e)$	$a(H_f)$	EPR-type
	DME		
203	0.372, 0.342, 0.321	0.124, 0.102, 0.035	*M*
223	0.366, 0.337, 0.320	0.124, 0.101, 0.035	*M*
243	0.361, 0.333, 0.317	0.121, 0.096, 0.035	*M*
263	0.328	0.097	*S*
	THF		
203	0.366, 0.337, 0.318	0.120, 0.101, 0.038	*M*
223	0.357, 0.336, 0.318	0.113, 0.099, 0.039	*M*
243	0.333	0.098	*S*
263	0.331	0.098	*S*
	MTHF		
203	0.335	0.100	*S*
223	0.333	0.098	*S*
243	0.332	0.098	*S*
263	0.331	0.098	*S*

Table 5 ^{1}H Coupling constants of $\mathbf{1}^{\bullet-}$ (mT). Counterion: Cs^+, solvents: DME, THF, MTHF

T/K	$a(H_e)$	$a(H_f)$	EPR-Type
	DME		
203	0.375, 0.321	0.123, 0.034	*A*
223	0.370, 0.320	0.121, 0.034	*A*
243	0.364, 0.319	0.119, 0.035	*A*
263	0.354, 0.339, 0.317	0.116, 0.095, 0.035	*M*
	THF		
203	0.363, 0.324	0.114, 0.038	*A*
223	0.361, 0.323[a]	0.113, 0.099, 0.038	*M*
243	0.357, 0.322[a]	0.112, 0.096, 0.038	*M*
263	0.319	0.096	*S*
	MTHF		
203	0.323	0.098	*S*
223	0.323	0.098	*S*
243	0.321	0.098	*S*
263	0.322	0.098	*S*

[a] Third coupling constant enveloped by broad ENDOR lines.

Table 6 Selected ^{1}H-coupling constants (mT) of $\mathbf{2}^{\bullet-}$

	HMPA/DME, 233 K	MTHF/Cs, 243 K
a_{He}	0.303, 0.287[a]	0.303
a_{Hf}	0.137, 0.116, 0.055	0.115
a_N	*b*	0.087, 0.067
EPR-Type	*M*	*S*

[a] Third coupling constant in this region enveloped by broad ENDOR lines. [b] ^{14}N Coupling constant not determined.

Table 7 ^{7}Li and ^{133}Cs coupling constants (mT) in MTHF

	$\mathbf{1}^{\bullet-}$		$\mathbf{2}^{\bullet-}$	
T/K	a_{Li}	a_{Cs}	a_{Li}	a_{Cs}
223	0.016	—	—	0.0065
243	0.014	0.047	—	0.0085
263	0.013	0.040	—	0.0095

Temperature Dependence of the EPR Spectra. Furan Derivative $\mathbf{1}^{\bullet-}$.—In the EPR spectra of $\mathbf{1}^{\bullet-}$ in DME/HMPA 5:1 (reduction with K or Cs), the coupling constants are nearly temperature-independent (Table 1, Fig. 6); there are only minor changes, *i.e.*, a decrease of a_{He} from 0.382 to 0.365 and from 0.314 to 0.307 mT. The values of a_{Hf} shift from 0.130 to 0.123 mT or from 0.026 to 0.030 mT on raising the temperature from 203 to 263 K. The same behaviour was found when **1** was reduced with Zn in a DMF solution. The multiplicities of the coupling constants remained unchanged over the whole temperature range.

With Li^+ as counterion (Table 2, Fig. 6) in DME and THF, type *A* spectra were observed from 203 to 228 K, then changing to *M* and to *S* above 253 K. The EPR spectra taken in MTHF were of type *S* in the whole temperature range studied.

Na^+ as the counterion (Table 3, Fig. 6) gave rise to type *M* spectra in DME from 203–253 K followed by type *S* at higher temperatures. In THF and MTHF as the solvents, only type *S* spectra were measured.

The coupling constants taken from the EPR spectra with K^+ as the counterion indicated type *M* in DME from 203 to 253 K and in THF from 203 to 233 K. The EPR spectra were of type *S* in DME above 253, in THF above 233 K and over the whole temperature range in MTHF as the solvent (Table 4, Fig. 6).

The EPR spectra of $\mathbf{1}^{\bullet-}/Cs^+$ remain type *A* in DME up to 253 K and in THF to 218 K, type *M* in DME above 253 K and in THF from 218 to 248 K. Type *S* is detected in THF above 248 K and in MTHF in the whole temperature range (Table 5, Fig. 6).

Thiophene Derivative $\mathbf{2}^{\bullet-}$.—For $\mathbf{2}^{\bullet-}$, only spectra of types *M* and *S* were recorded. Using a HMPA/DME mixture as the solvent, only *M*-type spectra were observed. Change to DME led to *M*-type spectra, which, using K^+ or Na^+ as counterions, turned to *S*-type above 248 K. In THF, with Li^+, *M*-type spectra prevailed, whereas with Cs^+, K^+ and Na^+, the EPR-spectra were of type *S*. In MTHF, only type *S* spectra could be discerned except for Li^+, where *M*-type spectra were detected over the whole temperature range (Fig. 6).

For both radical anions, $\mathbf{1}^{\bullet-}$ and $\mathbf{2}^{\bullet-}$, the temperature-dependent changes of the EPR spectra occurred within a range of *ca.* 10 K, thus, the temperatures given in the text and in Fig. 6 possess a margin of ±5 K.

Discussion

EPR Spectra and Molecular Symmetry.—The EPR spectra of type *A* and *S* can be related to different symmetries (conformations) and ion pairs of $\mathbf{1}^{\bullet-}$ and $\mathbf{2}^{\bullet-}$ which are listed in Table 8.

However, the alternations between *A* and *S* (*via M*) are closely connected to the solvent properties. Consequently, only a limited number of the structures given in Table 8 have to be considered.

(i) The observation of *A*-type spectra is limited to polar solvents which impair contact ion-pair formation, in particular DME/HMPA or DMF. The EPR spectra remain type *A* even at high temperatures. This observation mirrors the presence of solvent separated (free) ions[16] which do not change the symmetry upon temperature variation.* The number of coupling constants is four, each belonging to one single proton. Thus, the EPR signal is split into four sets of doublets by the ^{1}H coupling constants and the central line vanishes. This pattern indicates C_s symmetry (conformation: *syn*/*anti*, Fig. 1; bold face in Table 8).

(ii) Type *S* spectra were recorded when less polar solvents (DME ⟶ THF ⟶ MTHF) and/or higher temperatures (to lower the polarity of the solvent) were employed. These conditions strongly favour the formation of contact ion-pairs. Thus, two a_H (belonging to two pairs of protons) imply C_{2v} symmetry of a contact ion-pair (conformations *syn*/*syn* or *anti*/*anti*, Fig. 1; bold face in Table 8).

(iii) A third kind of EPR spectrum is recorded when those of type *A* and *S* are superimposed. Owing to small differences in the *g* factors of the *A*- and *S*-type spectra, the low- and high-field halves do not correspond to each other and no central line is visible. This situation is represented by EPR spectra of type *M* and indicates a mixture in which two conformers of different symmetry coexist [(*syn*/*syn*)/(*syn*/*anti*) or (*anti*/*anti*)/(*syn*/*anti*), see Fig. 1].

The ion pair structures connected with the EPR spectra of type *S* are discussed in the next section.

Contact Ion-pair Structures.—According to HMO calculations, the highest negative π-charge excess exists at the four N-atoms of the CN groups. Therefore, the alkali-metal counterion

* For the thiophene derivative $\mathbf{2}^{\bullet-}$ no spectra of type *A* were detected (see Fig. 6). This can be explained by a lower rotational barrier for the change from a *syn*/*anti* to a *syn*/*syn* conformation for $\mathbf{2}^{\bullet-}$ than for $\mathbf{1}^{\bullet-}$. This behaviour is also indicated by AM1[17] calculations.

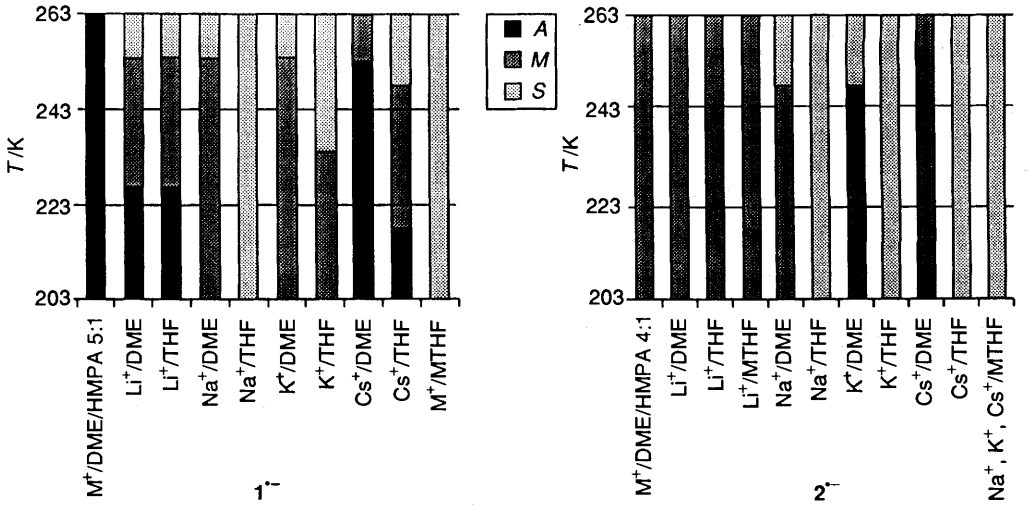

Fig. 6 Stack-diagram of temperature, solvent and alkali-metal counterion dependence of the EPR spectra according to the types *A*, *M*, *S*: left; $\mathbf{1}^{\bullet -}$, right $\mathbf{2}^{\bullet -}$

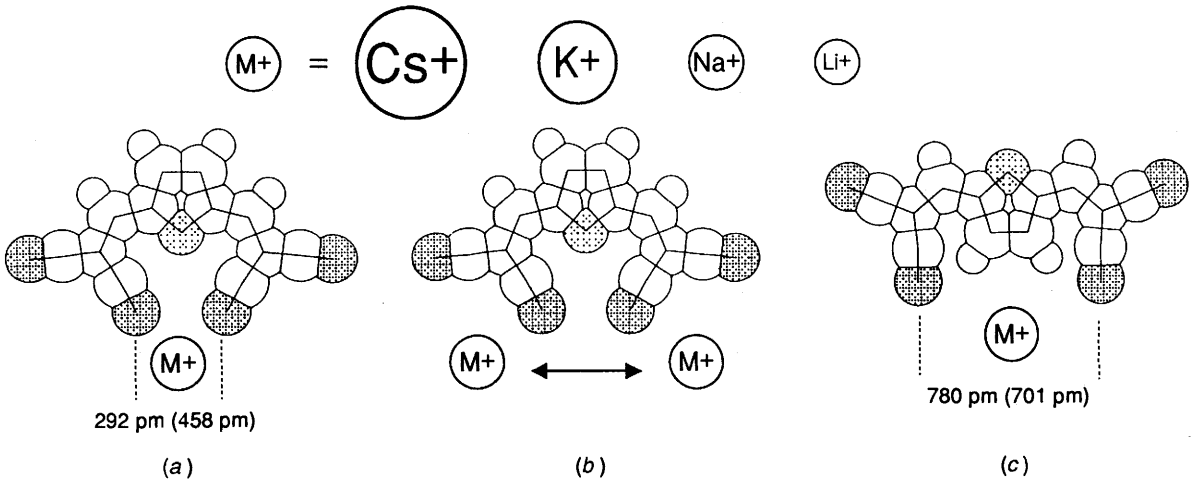

Fig. 7 Three contact ion-pairs of $\mathbf{1}^{\bullet -}$ ($\mathbf{2}^{\bullet -}$)/[metal]$^+$; the counterions M^+ are positioned in the horizontal nodal plane of the π-system of **1** (**2**)

Table 8 Structures of $\mathbf{1}^{\bullet -}$ or $\mathbf{2}^{\bullet -}$ which could be related to EPR spectra of type *A* or *S*. The possibilities which are compatible with the experiment and are discussed in the text are given in bold face

Spectrum type	Conformation	Free ion/contact ion-pair	Remarks
A	***syn/anti***	**Free ion**	**One conformation**
	syn/anti	Contact ion-pair	—
	syn/syn	Contact ion-pair	Association lowering symmetry
	anti/anti	Contact ion-pair	Association lowering symmetry
S	—	Free ion	Free rotation of the C=C(CN)$_2$ groups, fast on the hyperfine time-scale
	syn/syn	Free ion	—
	anti/anti	Free ion	—
	syn/syn	**Contact ion-pair**	**M^+ on the C_2 axis**
	syn/syn	**Contact ion-pair**	**Fast exchange of M^+ between equivalent positions** [*cf.* Fig. 7(*b*)]
	anti/anti	**Contact ion-pair**	**M^+ on the C_2 axis**
	anti/anti	**Contact ion-pair**	**Fast exchange of M^+ between equivalent positions** [*cf.* Fig. 7(*b*)]

should preferably be associated to some of these N-atoms. The finding that it was possible to measure only rather low metal coupling constants (*ca.* 0.014 mT for $\mathbf{1}^{\bullet -}/Li^+$ and 0.007–0.047 mT for $\mathbf{1}^{\bullet -}$ and $\mathbf{2}^{\bullet -}/Cs^+$; Table 7) or none ($K^+$, Na^+) even in a nonpolar solvent like MTHF, indicates that the metal ions should reside in the horizontal nodal plane of the π system of $\mathbf{1}^{\bullet -}$ or $\mathbf{2}^{\bullet -}$[4] (averaged on the hyperfine time-scale).

With these limitations taken into account, four different contact ion-pair structures of $\mathbf{1}^{\bullet -}$ ($\mathbf{2}^{\bullet -}$)/[metal]$^+$ giving rise to the observed spectral features have to be considered (Fig. 7). The alkali-metal cation could oscillate between two equivalent dicyanomethylidene moieties of structure (i) *syn/syn* or (ii) *anti/anti* (Fig. 1) as shown in Fig. 7(*b*) for *syn/syn*, the exchange rate being fast on the hyperfine time-scale. (iii) With the *anti/anti* conformation (Fig. 1) of $\mathbf{1}^{\bullet -}$ and $\mathbf{2}^{\bullet -}$, the site to accommodate the counterion is situated between the two N-atoms pointing to

the H-atoms at the 3 and 4 positions of the furan (thiophene) ring [Fig. 7(*c*)]. (iv) When conformation *syn/syn* is preferred, the metal cation could also be positioned between the two N-atoms facing the furan (thiophene) O–(S)-atom [Fig. 7(*a*)].

The distances between the facing N-atoms of the dicyanoethene moieties, calculated by the UHF–AM1 method,[17] are as follows: for the *syn/syn* isomers the N···N distance increases from 292 pm for $\mathbf{1}^{\bullet-}$ to 458 pm for $\mathbf{2}^{\bullet-}$; the corresponding values for the *anti/anti* conformers are 780 pm and 701 pm for $\mathbf{1}^{\bullet-}$ and $\mathbf{2}^{\bullet-}$, respectively (Fig. 7). The ionic radii of Li^+, Na^+, K^+ and Cs^+ are *ca.* 60, 95, 133 and 169 pm, respectively (however, these radii depend on the solvent).[18] From the N···N distance and the size of the alkali-metal cations an ion pair as depicted in Fig. 7 (*c*) is unlikely because (i) the two N-atoms being more than 700 pm apart are not a good chelating group for the cations and (ii) the differences between the temperature, solvent, and counterion dependent types of spectra for $\mathbf{1}^{\bullet-}$ and $\mathbf{2}^{\bullet-}$ should not be that significant.

The following additional findings help to distinguish between the structures (*a*) and (*b*) in Fig. 7. The ion pair of type (*b*) is of the same kind as an ion pair of tetracyanoquinodimethane (TCNQ) having similar charge-excess values at the N-atoms as $\mathbf{1}^{\bullet-}$ and $\mathbf{2}^{\bullet-}$. Thus, $TCNQ^{\bullet-}$/[metal]$^+$ should reveal the same behaviour as found for the ion pairs of $\mathbf{1}^{\bullet-}$ and $\mathbf{2}^{\bullet-}$. The radical anion of TCNQ is well known,[19] nevertheless we did not find data with $^7Li^+$ or $^{133}Cs^+$ ion pairs of $TCNQ^{\bullet-}$. In a re-examination of $TCNQ^{\bullet-}$ in MTHF as the solvent, no ^7Li or ^{133}Cs coupling constants were detected, either by EPR or by ENDOR spectroscopy. The EPR spectra were invariant to temperature changes and identical, both with Li^+ and Cs^+, to those published with K^+ as the counterion.[19] This observation excludes the structure (*b*) depicted in Fig. 7 to be a correct model for the ion pair of $\mathbf{1}^{\bullet-}$ ($\mathbf{2}^{\bullet-}$)/[metal]$^+$. Furthermore, for both, the furan and the thiophene derivative, the dicyanomethylidene moieties possess nearly identical structures. Thus, an ion pair of type (*b*), where the metal cations are complexed by the two N-atoms of one dicyanomethylidene group, does not account for the different behaviour of $\mathbf{1}^{\bullet-}$ and $\mathbf{2}^{\bullet-}$.

Thus only the structure according to (*a*) (Fig. 7) remains as a plausible model for the contact ion-pair of $\mathbf{1}^{\bullet-}$ ($\mathbf{2}^{\bullet-}$)/[metal]$^+$. The N···N distances of 292 ($\mathbf{1}^{\bullet-}$) and 458 pm ($\mathbf{2}^{\bullet-}$) are of a similar order of magnitude as those in tetramethylethylenediamine[20] or 2,2′-bipyridyl[21] which are known as suitable ligands for alkali-metal cations. Regarding Fig. 6, one can see that in the case of $\mathbf{1}^{\bullet-}$ Na^+ has the strongest tendency to produce EPR spectra of type *S* (C_{2v} symmetric ion pair) even at low temperatures with a solvent of strong alkali-metal solvating power (DME), followed by K^+, Li^+ and Cs^+; this order is changed to K^+, $Cs^+ > Na^+ > Li^+$ for the thiophene compound $\mathbf{2}^{\bullet-}$.

The preference of smaller cations for $\mathbf{1}^{\bullet-}$ and bigger ones for $\mathbf{2}^{\bullet-}$ is in line with the different N···N distances of the facing N-atoms stemming from the two different dicyanoethene moieties, *i.e.* 292 pm in $\mathbf{1}^{\bullet-}$ and 458 pm in $\mathbf{2}^{\bullet-}$ (Fig. 7). Whereas the greater N···N distance in $\mathbf{2}^{\bullet-}$ impairs the formation of a Li^+ contact ion-pair even in MTHF (Fig. 6), the preferred complexation of K^+ and Cs^+ by $\mathbf{2}^{\bullet-}$ may additionally serve as evidence of a contribution of the thiophene S-atom ('soft' Lewis base) as a part of the chelating ligand to the 'soft' alkali metals K^+ and Cs^+.

The Kinetics of the Structural Change.—In the temperature range where conformational changes take place, line broadening (alternating line widths) is observed in the EPR spectra.[22] However, in the EPR spectra of $\mathbf{1}^{\bullet-}$ and $\mathbf{2}^{\bullet-}$ the small changes of the ^1H coupling constants from 0.37/0.32 to 0.35 mT for a_{He} and from 0.125/0.035 to 0.100 mT for a_{Hf} ($\mathbf{1}^{\bullet-}$; the differences for $\mathbf{2}^{\bullet-}$ being even smaller), together with the low rotational barriers between the *syn/anti* and *syn/syn* conformations (see below), lead to a rather narrow temperature range for line-width alternation (*ca.* 10 K, see results). Moreover, due to broad lines, an unambiguous simulation of the *M*-type spectra was not possible. Thus, only an estimate of the free enthalpy of activation can be given. According to the formula[23] $\Delta G_{Tc}^{\ddagger} = 19.13\ T_c(9.97 + \log T_c/\Delta\nu)$ [J mol^{-1}], where T_c is the coalescence temperature and $\Delta\nu$ is the difference of the proton-hyperfine splittings in Hz. With $T_c = 253 \pm 10$ K (*M* to *S* type EPR spectrum for $\mathbf{1}^{\bullet-}$ in DME with Li^+, Na^+, or K^+ as counterion) and $\Delta\nu = 1.4 \pm 0.1$ MHz (0.05 mT), $\Delta G_{253}^{\ddagger} \approx 30 \pm 2$ kJ mol^{-1} is obtained.

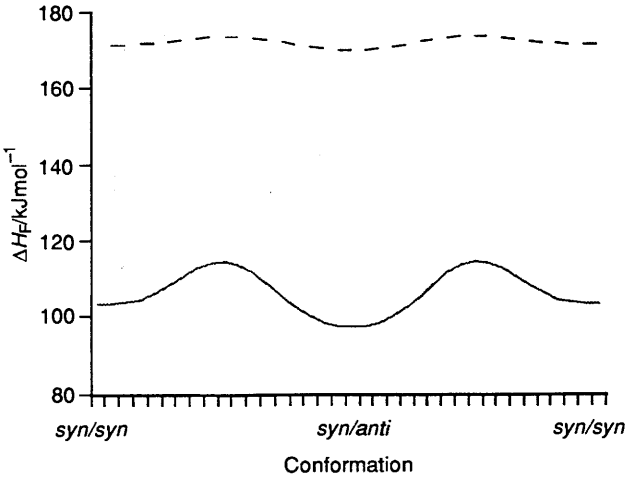

Fig. 8 Profiles of the rotation from a *syn/syn* to a *syn/anti* conformation for **1** (– – –) and $\mathbf{1}^{\bullet-}$ (——) calculated by AM1

Remarks about Rotational Barriers and Coulomb Interactions.—As shown in the previous section, the contact ion-pair formation process in the radical anions $\mathbf{1}^{\bullet-}$ and $\mathbf{2}^{\bullet-}$ is connected with a rotation around a bond between the furan (thiophene) fragment and the dicyanoethene moiety. This rotation has a significantly lower barrier in the neutral molecules **1** and **2** than in the radical anions $\mathbf{1}^{\bullet-}$ and $\mathbf{2}^{\bullet-}$ owing to an increase of the order of the corresponding bond as shown in Fig. 8 for **1** and $\mathbf{1}^{\bullet-}$. The low barriers between the planar *syn/anti* and *syn/syn* structures of neutral **1** and **2** are mirrored by their ^1H-NMR spectra which show signals belonging to two pairs of equivalent protons.[24] The increase of the bond order in the radical anions together with the use of the 'faster' EPR hyperfine time-scale leads to the observation of three EPR spectral types corresponding to the existence of two different conformers of $\mathbf{1}^{\bullet-}$ and $\mathbf{2}^{\bullet-}$. The fact that for $\mathbf{2}^{\bullet-}$ no spectra of type *A* were detected is in line with AM1[17] calculations. These indicate a lower rotational barrier for the thiophene derivative $\mathbf{2}^{\bullet-}$ than for $\mathbf{1}^{\bullet-}$. Therefore, for $\mathbf{2}^{\bullet-}$ a mixture of *syn/syn* and *syn/anti* conformations is detected even at low temperatures and without the formation of contact ion-pairs (Fig. 6).

It is well established that the interactions between radical ions and their counterions are dominated by Coulomb-type interactions.[25] To effect a change between a *syn/anti* and a *syn/syn* conformation, the coulomb energy has to exceed the barrier between these conformations. To get an estimate of the distance between the radical anion and the alkali-metal cation one could simply use the AM1-calculated rotational barriers and the relative permittivities of DME,[26] THF[26] or MTHF[27] at the temperatures where a change from *A*- to *S*-type EPR spectra occurs. However, care must be taken when using the calculated rotational barriers and the macroscopic permittivities: (i) the calculated rotational barrier in *e.g.* Fig. 8 does not take into account interactions between the charged radical ions and the dipoles of the solvent molecules which possibly lead to an increase of these barriers; (ii) the macroscopic permittivity of the solvents is higher than the effective microscopic value.

Thus, although it is tempting to derive anion/cation distances of contact ion-pairs in solution from experimental data and calculated energies, further knowledge about the molecular interactions is necessary to get more insight into the structures and energies of ion pairs.

Conclusions

For either of the radical anions $\mathbf{1}^{\bullet-}$ and $\mathbf{2}^{\bullet-}$ an increase of molecular symmetry upon conditions favouring contact ion-pairs was observed. The EPR hyperfine data support the ion-pair structure shown in Fig. 7(*a*) as the most plausible.

The ion-pair formation can not be attributed to concentration phenomena because the EPR-spectral alternations were neither dependent on the concentration of the radical ions nor on the grade of reduction (time of the contact of the solutions containing the neutral species with the alkali-metal mirrors or amount of LiCl added, see the Experimental section).

Regarding Figs. 6 and 7, the Na^+ has the strongest effect to produce a C_{2v}-symmetric ion pair with $\mathbf{1}^{\bullet-}$, followed by K^+, Li^+ and Cs^+; for $\mathbf{2}^{\bullet-}$ the order is K^+, $Cs^+ > Na^+ > Li^+$. The preference of $\mathbf{1}^{\bullet-}$ to form contact ion-pairs with 'hard' (Li^+, Na^+) and of $\mathbf{2}^{\bullet-}$ with 'soft' Lewis acids points to an additional participation of the five-ring heteroatoms O and S to the complexation of the alkali-metal counterions.

It is noteworthy that contact ion-pair formation 'increases' the molecular symmetry. Thus it became possible to observe the effect of the counterion on the structure of $\mathbf{1}^{\bullet-}$ and $\mathbf{2}^{\bullet-}$ just by the change of the multiplicities of the ^1H coupling constants and without the necessity to detect an alkali-metal coupling constant.

Acknowledgements

We gratefully acknowledge the support by the *Schweizerischer Nationalfonds zur Förderung der wissenschaftlichen Forschung* (M. S. and G. G.) and the *Bundesminister für Forschung und Technologie* (U. S. and J. D.).

References

1 J. Daub, K. M. Rapp, J. Salbeck and U. Schöberl in *Carbohydrates as Organic Raw Materials*, ed., W. Lichtenthaler, VCH Publishers, Weinheim, New York, 1991.
2 J. Salbeck, U. Schöberl, K. M. Rapp and J. Daub, *Z. Phys. Chem.*, 1991, **171**, 191.
3 R. Schenk, W. Huber, P. Schade and K. Müllen, *Chem. Ber.*, 1988, **121**, 2201; W. Huber and K. Müllen, *Acc. Chem. Res.*, 1986, **19**, 300.
4 T. Takeshita and N. Hirota, *J. Am. Chem. Soc.*, 1971, **93**, 6421; N, Hirota in *Radical Ions*, eds., E. T. Kaiser and L. Kevan, Wiley Interscience, New York, London, Sydney, 1968.
5 *Ions and Ion Pairs in Organic Reactions*, Parts 1 and 2, ed., M. Szwarc, Wiley, New York, 1972 and 1974.
6 M. Barzaghi, S. Miertus, C. Oliva, E. Ortoleva and M. Simonetta, *J. Phys. Chem.*, 1983, **87**, 881; G. A. Russell, J. L. Gerlock and D. F. Lawson, *J. Am. Chem. Soc.*, 1971, **93**, 4088; G. A. Russell, D. F. Lawson, H. L. Malkus, R. D. Stephens, G. R. Underwood, T. Takano and V. Malatesta, *J. Am. Chem. Soc.*, 1974, **96**, 5830; E. W. Stone and A. H. Maki, *J. Chem. Phys.*, 1963, **38**, 1999.
7 M. Candida, B. Loia, B. J. Herold, N. M. Atherton and H. M. Novais, *J. Chem. Soc., Faraday Trans. 2*, 1981, **77**, 1643; N. M. Atherton, B. J. Herold, M. Celina, R. Lazana, M. Candida and B. Shohoji, *J. Chem. Soc., Faraday Trans. 2*, 1982, **78**, 1781.
8 W. Lubitz, M. Plato, K. Möbius and R. Biehl, *J. Phys. Chem.*, 1979, **83**, 3402.
9 (*a*) R. Borghi, M. A. Cremonini, L. Lunazzi, G. Placucci and D. Macciantelli, *J. Org. Chem.*, 1991, **56**, 6337; (*b*) M. Guerra, G. Pedulli and M. Tiecco, *J. Chem. Soc., Perkin Trans. 2*, 1973, 903.
10 H. Kurreck, B. Kirste and W. Lubitz, *Electron Nuclear Double Resonance Spectroscopy of Radicals in Solution*, VCH Publishers, Weinheim, New York, 1988.
11 K. P. Dinse, R. Biehl and K. Möbius, *J. Chem. Phys.*, 1974, **61**, 4335; R. Biehl, M. Plato and K. Möbius, *J. Chem. Phys.*, 1975, **63**, 3515.
12 A. D. McLachlan, *Mol. Phys.*, 1960, **3**, 233.
13 F. Gerson, *High Resolution E.S.R. Spectroscopy*, Wiley and Verlag Chemie, New York and Weinheim, 1970.
14 L. Cavara, F. Gerson, D. O. Cowan and K. Lerstrup, *Helv. Chim. Acta*, 1986, **69**, 141.
15 E. Heilbronner and H. Bock, *The HMO-Model and its Application*, Wiley and Verlag Chemie, London, New York and Weinheim, 1976.
16 C. Reichardt, *Solvents and Solvent Effects in Organic Chemistry*, 2nd edn., VCH, Weinheim, 1990, chapter 2.6, p. 47.
17 M. J. S. Dewar, E. G. Zoebisch, E. F. Healy and J. J. P. Stewart, *J. Am. Chem. Soc.*, 1985, **107**, 3902.
18 P. M. Qureshi and I. M. Kamoonpuri, *J. Chem. Educ.*, 1991, **68**, 109; M. Szwarc, in ref. 5, chapter 1.
19 M. L. Kaplan, R. C. Haddon, F. B. Bramwell, F. Wudl, J. H. Marshall, D. O. Cowan and S. Gronowitz, *J. Phys. Chem.*, 1980, **84**, 427; A. M. Kini, D. O. Cowan, F. Gerson and R. Möckel, *J. Am. Chem. Soc.*, 1985, **107**, 556; P. H. Rieger and G. K. Fraenkel, *J. Chem. Phys.*, 1962, **37**, 2795.
20 D. Seebach, R. Amstutz, T. Laube, W. B. Schweizer and J. D. Dunitz, *J. Am. Chem. Soc.*, 1985, **107**, 5403; D. Seebach and Th. Maetzke, *Helv. Chim. Acta*, 1989, **72**, 624.
21 L. Echegoyen, A. DeCian, J. Fischer and J. M. Lehn, *Angew. Chem., Int. Ed. Engl.*, 1991, **30**, 838.
22 Ref. 13, chapter A.2.3.
23 H. Günther, *NMR-Spektroskopie*, G. Thieme Verlag, Stuttgart, New York, 1983, p. 229.
24 U. Schöberl, Ph.D. Thesis, Regensburg, 1991.
25 Ref. 16, chapter 2.6, p. 42.
26 P. Chang, R. V. Slates and M. Szwarc, *J. Phys. Chem.*, 1966, **70**, 3180.
27 C. Carvajal, K. J. Tölle, J. Smid and M. Szwarc, *J. Am. Chem. Soc.*, 1965, **87**, 5548.

Paper 2/04188J
Received 4*th August* 1992
Accepted 19*th August* 1992